# Apodization Method in UWB SAR Imaging

Habiba Akhter
Department of Electrical Engineering
Blekinge Institute of Technology
Karlskrona, Sweden
habiba.khandaker@yahoo.com

***Abstract*—Synthetic Aperture Radar (SAR) image processing involves a two dimensional (2-D) Fourier Transform (FT) and the spectrum shape introduces high intensity sidelobes. These sidelobes may severely distort the image. Apodization technique can decrease the sidelobes level while preserving the image resolution. However, in Ultra wideband (UWB) SAR imaging, we have to reduce both orthogonal and non-orthogonal sidelobes. In this paper, a new linear window function has been presented based on analysis of different linear and non-linear apodization techniques. This new linear method controls both orthogonal and non-orthogonal sidelobes better than other conventional window functions. This method has been applied and verified with a real SAR image.**

***Keywords- Apodization, image resolution, sidelobe, synthetic aperture radar (SAR).***

## I. INTRODUCTION

Synthetic Aperture Radar (SAR) is unique in its imaging capability. One of the research interests is to improve resolution of SAR images as spaceborne and airborne SAR techniques are growing. Conventional Fourier Transform (FT) based image reconstruction techniques in SAR and inverse SAR (ISAR) image provides limited resolution. Moreover, conventional SAR image processing system involves a two-dimensional (2-D) FT that can produce significant high intensity sidelobes. Apodization technique is used in SAR images to suppress the sidelobes.

Apodization technique is done by applying two-dimensional window functions to the spectrum of SAR images. This technique is known as rectangle approximation which is suitable for narrowbeam-narrowband (NB) SAR images and induces only orthogonal sidelobes. Ultra wideband (UWB) SAR system utilizes large integration angle and relative large bandwidth and therefore, introduces both orthogonal and non-orthogonal sidelobes. The sidelobes in azimuth and slant range can be suppressed by 2-D window functions in SAR image spectrum, but it also reduces resolution. Linear window functions can control the sidelobes level, and trade against loss in resolution, whereas non-linear window functions can enhance resolution as well as control sidelobes. However, it is hard to identify the relation between the apodized image and the real image considering the properties of objects in the image. In these aspects, it is important to control sidelobes and preserves good resolution at the same time using linear apodization method. Moreover, it is mainly of interest to relate it to UWB SAR where not enough research has been done on linear apodization.

In this paper, different window methods have been investigated and comparison is made in terms of resolution loss and orthogonal and non-orthogonal sidelobes reduction. The paper is organized as follows: section II introduces conventional apodization methods, section III briefly describes the method to measure the resolution of UWB SAR image, section IV provides proposed window function and simulation results and section V concludes the paper.

## II. APODIZATION TECHNIQUES

Some popular window functions have been illustrated here. Rectangle window can be expressed as,

$$w_{rec}(n) = 1 \tag{1}$$

The Hamming window is widely used in many applications e.g. speech processing. This window has shape of

$$w_{hm}(n) = \begin{cases} 0.54 - 0.46\cos\left(\frac{2\pi n}{M}\right) & 0 \le n \le M \\ 0 & else \end{cases} \tag{2}$$

The Hanning window function,

$$w_{hn}(n) = \begin{cases} 0.5(1 - \cos\left(\frac{2\pi n}{N-1}\right)) & 0 \le n \le M \\ 0 & else \end{cases} \tag{3}$$

The Blackman window function,

$$w_{blk}(n) = \begin{cases} a_0 - a_1\cos\left(\frac{2\pi n}{N-1}\right) + a_2\cos\left(\frac{4\pi n}{N-1}\right) & 0 \le n \le M \\ 0 & else \end{cases} \tag{4}$$

where $a_0 = \frac{1-\alpha}{2}$, $a_1 = \frac{1}{2}$, $a_2 = \frac{\alpha}{2}$ and $\alpha = 0.16$

The kaiser window provides better sidelobes reduction and achieves high image resolution in some cases compared to SVA [1]. This window can be illustrated as

$$w_k(n) = \begin{cases} \frac{I_0\left[\beta\left(1-[(n-\frac{M}{2})/(M/2)]^2\right)^{0.5}\right]}{I_0(\beta)} & 0 \le n \le M \\ 0 & else \end{cases} \quad (5)$$

where $I_0$ is the zero order Bessel function and β is a tuning parameter which estimates the 'mainlobe width – sidelobe peak' tradeoff.

SVA (cosine-on-pedestal) is used in dynamic window functions and is very easy for estimation. The window function of SVA is:

$$w(n) = 1 + 2w\cos(2\pi\frac{n}{N}) \quad (6)$$

The window factor w can have values from 0 (i.e. Rectangle) to 0.5 (i.e. Hanning) [2].

## III. SAR IMAGE QUALITY MEASUREMENT

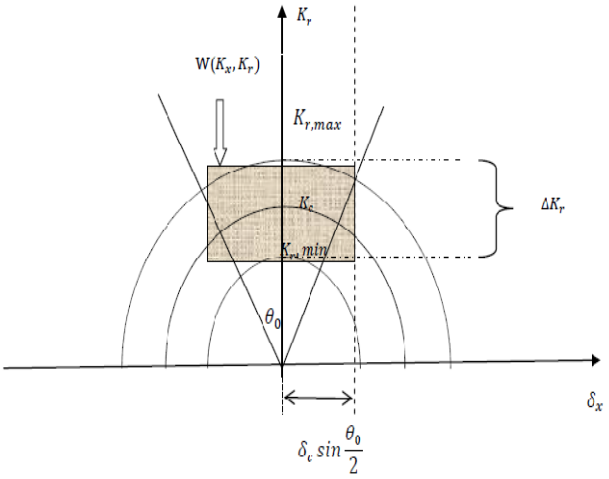


Fig. 1. An example of implementing Rectangle window (shaded area) in wave domain

In Fig. 1, the range wave number $k_r$ , the azimuth wave number $k_x$ and the radar frequency w are related together as [3]

$$w = \frac{c}{2}\sqrt{k_r^2 + k_x^2} \quad (7)$$

where c is speed of light.

$$\text{and } \Delta K_r = K_{r,max} - K_{r,min} \quad (8)$$

where $K_{r,max}$ and $K_{r,min}$ are maximum and minimum range wave numbers, respectively.

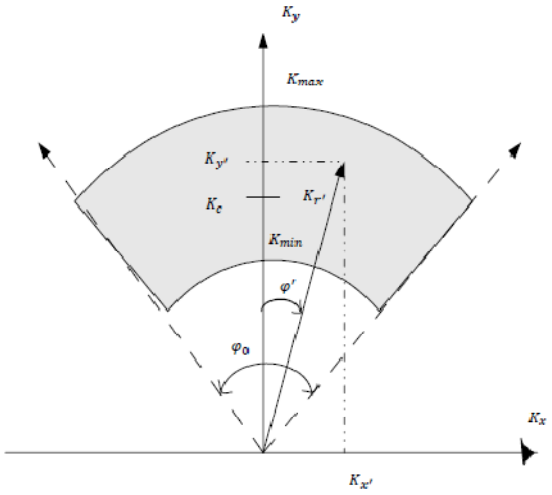


Fig. 2. SAR spectrum in wave domain

In Fig. 2, $K_c$ and $\varphi_0$ are centre wavelength and integration angle of a SAR system, respectively. $K_{min}$ and $K_{max}$ are the wave numbers corresponding to the lowest and highest signal frequencies.

The signal bandwidth $B_r$ can be illustrated as [4],

$$B_r = (K_{max} - K_{min})/K_c \quad (9)$$

Impulse Response Function (IRF) is strongly related to the measurements of SAR image resolution and evaluation of the quality of SAR images [5]. Generally 2-D *sinc* function $(\sin(x)/x)$ is utilized as IRF in SAR image formation which is achieved through rectangle estimation for 2-D SAR spectrum. On the basis of flat spectrum, $H(K_x, K_r)$ can be illustrated as

$$H(K_x, K_r) \approx \begin{cases} 1 & K_{x,min} \le K_x \le K_{x,max} \\ & K_{r,min} \le K_r \le K_{r,max} \\ 0 & elsewhere \end{cases} \quad (10)$$

The 2-D Inverse Fourier Transform (IFT) of spectrum $H(K_x, K_r)$ can be written as [6].

$$h(x,r) = \int_{-\infty}^{+\infty}\int_{-\infty}^{+\infty} H(K_x, K_r).e^{i(K_x x + K_r r)}dK_x dK_r \quad (11)$$

A 2-D *sinc* function has been demonstrated in [5] which is approximated from equation (10) for IRF SAR in both range and azimuth directions.

$$h(x,r) \approx sinc\left(k_{r,c}xsin\frac{\theta_0}{2}\right).sinc\left(\frac{k_{r,max}-k_{r,min}}{2}r\right) \quad (12)$$

where $\theta_0$ is an integration angle and $k_{r,c}$ is the centre wave number. This function is applicable for NB SAR system.

The maximum integration angle, bandwidth respectively $\theta \leq 10^{\circ}$ and $B_r \geq 0.2$ are suitable for NB SAR [4]. For wide integration angle ($\theta \approx 110^{\circ}$) and large bandwidth ($B_r \approx 1.1$) this *sinc* function cannot be applicable.

A new IRF SAR is illustrated in [5],

$$h(v_t, \varphi_t, B_r, \theta_0) = \frac{e^{-i\varphi t}}{v_t}\left[\frac{i^n h_{1,n-1}(v_t, B_r)}{e^{i(n-1)\varphi_t}} sinc\left(n\frac{\theta_0}{2}\right)\right] + \frac{e^{-i\varphi t}}{v_t} h_2(v_t, \varphi_t, B_r, \theta_0) \quad (13)$$

where

$$h_{1,n-1}(v_t, B_r) = -(1+\tfrac{B_r}{2})\, J_{n-1}\,[v_t(1+\tfrac{B_r}{2})] + (1-\tfrac{B_r}{2})\, J_{n-1}[v_t(1-\tfrac{B_r}{2})] \quad (14)$$

$$h_2(v_t, \varphi_t, B_r, \theta_0) = -B_r sinc\left[\frac{B_r}{2} v_t cos\left(\frac{\theta_0}{2} + \varphi_t\right)\right] e^{iv_t \cos\left(\frac{\theta_0}{2}+\varphi_t\right) - i\frac{\theta_0}{2}} + B_r sinc\left[\frac{B_r}{2} v_t cos\left(\frac{\theta_0}{2} - \varphi_t\right)\right] e^{iv_t \cos\left(\frac{\theta_0}{2}-\varphi_t\right) + i\frac{\theta_0}{2}} \quad (15)$$

The derived IRF SAR (12) is applicable for UWB IRF SAR system. This approximation is also suitable for NB SAR. However, by this approximation we can evaluate mainlobe areas of several SAR systems to estimate Peak Sidelobe Ratio (PSLR) and Integrated Sidelobe Ratio (ISLR) in order to asses SAR image quality.

## IV. SIDELOBES SUPRESSION RESULTS

After applying different window functions in SAR data, we conclude the best one which suppresses the sidelobes level while maintaining the image resolution. The comparison is made using parameters according to different window functions as well as with different integration angles.

The proposed linear window function is,

$$w(k_x, k_r) = \left[\gamma_x - \alpha_k cos\left(\frac{2\pi(atan\frac{k_x}{k_r})}{\frac{\emptyset_0}{2}}\right) - \beta_k cos\left(\frac{6\pi(atan\frac{k_x}{k_r})}{\frac{\emptyset_0}{2}}\right)\right] \cdot \left[\gamma_r - \alpha_k cos\left(\frac{2\pi(\sqrt{k_x^2+k_y^2}-k_c)}{k_{max}-k_{min}}\right) - \beta_k cos\left(\frac{6\pi(\sqrt{k_x^2+k_y^2}-k_c)}{k_{max}-k_{min}}\right)\right] \quad (16)$$

where $\gamma_x = \gamma_r = 0.63$, $\alpha_k = 0.45$, $\beta_k = 0.002$, $\emptyset_0$ is integration angle, the range wave number is $k_r$ and the azimuth wave number is $k_x$. $K_{min}$ and $K_{max}$ are the wave numbers corresponding to the lowest and highest signal frequencies.

TABLE I
CARABAS-II PARAMETERS FOR SIMULATIONS

| Parameter | Values |
|---|---|
| The highest frequency processed $f_{max}$ | 90 MHz |
| The lowest frequency processed $f_{min}$ | 20 MHz |
| Platform speed *Vpl* | 130 m/s |
| Pulse Repetition Frequency (PRF) | 137 Hz |

This proposed window function suppresses both orthogonal and non-orthogonal sidelobes and preserves the image resolution better than conventional linear window functions. In this paper, we apply window not only in azimuth and slant range direction but also in angle direction that is quite new. The example of angle direction is shown in Fig. 2, where the window can be apply to the integration angle direction from $\theta'$ to $k_{r'}$. For an arbitrary point in the spectrum, $(k_{x'}, k_{y'})$, a change of variable to $(\varphi', k_{r'})$ can be obtained [4] by

$$(\varphi', k_{r'}) = (\text{atan}(k_x/k_y), \sqrt{k_r^2 + k_x^2}) \quad (17)$$

After applying window in angle direction, we observe that it efficiently suppresses sidelobe level and preserves image resolution as well.

In order to prove our proposed method correct, a real SAR image has been processed. We use CARABAS-II SAR data. The main parameters of this system are summarized in Table 1. Hamming window function, Hanning window function and proposed window function is used in our simulations.

For simulation, at first, we have generated spectrums using different integration angles with relative bandwidth. Second, we have applied two-dimensional inverse FT to the spectrum. Third, we have applied different windows in spectrums and measured azimuth and range resolution loss.

The shape of point targets is actually different in UWB SAR compared to NB SAR [3]. For this reason, the normal quality measurements such as Range and Azimuth Resolution, Integrated Sidelobe Ratio (ISLR) and Peak Sidelobe Ratio (PSLR) do not provide useful Information. As this aspect, contour plots are used for illustrations.

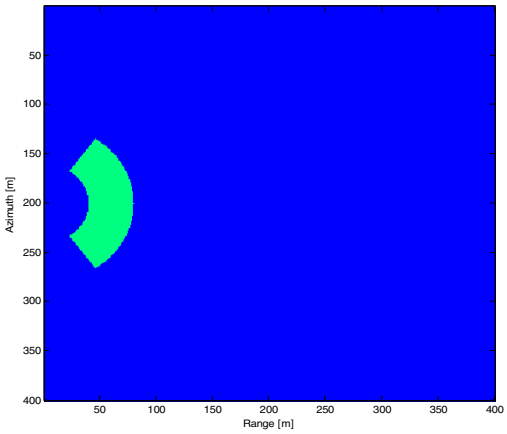


Fig. 3. SAR image spectrum (integration angle $\theta = 55^{\circ}$)

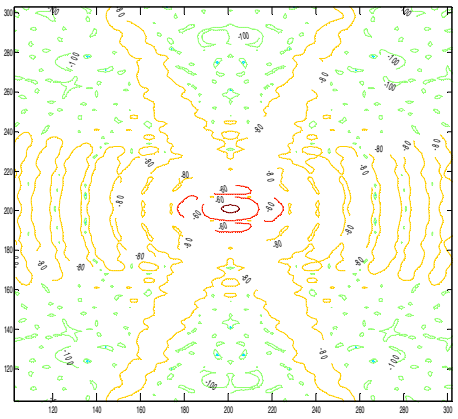

Fig. 4. Contour plot of non-apodized image in dB with different (10 to 110) integration angle

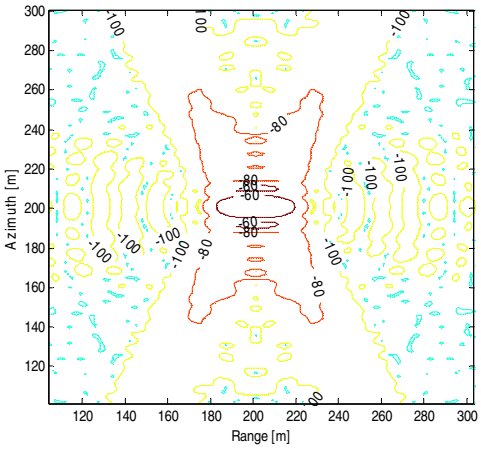


Fig. 5. Contour plot in dB by applying Hamming window function

Fig. 5 illustrates apodized image after implementing Hamming window function in azimuth direction. It can reduce orthogonal sidelobes but it induces resolution loss which is about 45%.

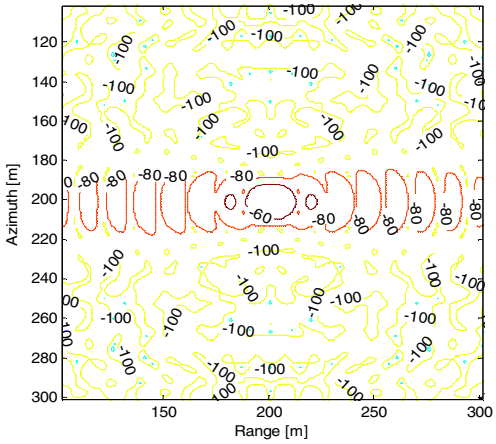


Fig. 6. Contour plot in dB by applying Hamming window function in angle direction

Fig. 6 illustrates apodized image after applying Hamming window function in angle direction. It reduces non-orthogonal sidelobes but it induces resolution loss which is about 45%.

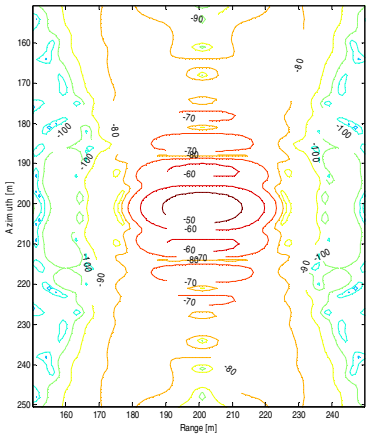


Fig. 7. Contour plot in dB by applying Hanning window function

Hanning window function is applied in azimuth direction in Fig. 7. It sufficiently suppressed orthogonal sidelobes with loss in resolution is about 60%.

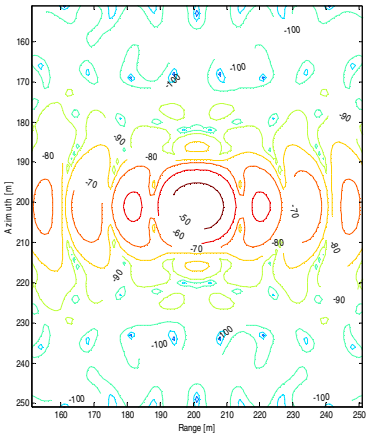


Fig. 8. Contour plot in dB by applying Hanning window function in angle direction

Hanning window function is applied in angle direction in Fig. 8. It sufficiently suppressed non-orthogonal sidelobes with 45% resolution loss.

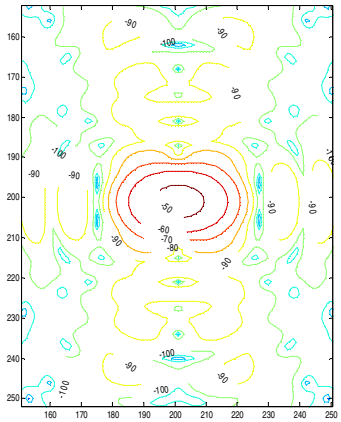

Fig. 9. Contour plot in dB by applying proposed window function

In Fig. 9, both orthogonal and non-orthogonal sidelobes are suppressed at desired level by applying new window function. The azimuth resolution loss is 33.34% and range resolution loss is 36.58% which are pretty less compared to traditional linear window function (e.g. Hamming, Hanning etc.) and it is nearly similar to Cosine-on-pedestal (about 33%).

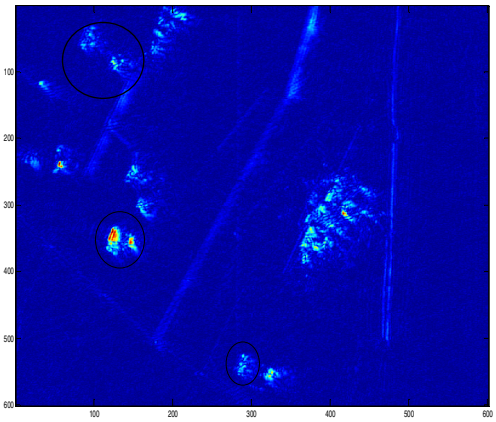

Fig. 10. Non-apodized real SAR image

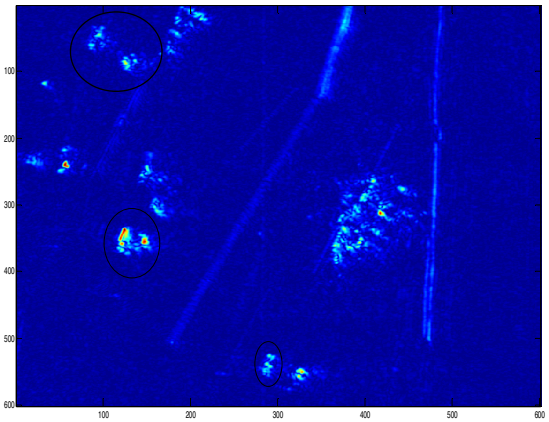

Fig. 11. Apodized real SAR image by applying proposed window function

Close observation on Fig. 10 and Fig. 11 exposes that applying this new window function clears the scattering areas of the image. All the major scattering centers are much better resolved by this new window function. Fig. 10 gives circle area which has the same scene as the Fig. 11. The Fig. 10 has some scattering areas, whereas Fig. 11 provides much better smooth and clear areas.

## V. CONCLUSION

The paper provides an efficient window function to enhance resolution as well as reduce sidelobes. The window is applied in azimuth, range and angle direction of UWB SAR image. After applying this window function in angle directions, it sufficiently suppresses the sidelobe level and provides better resolution than applying window function in azimuth or range direction only. This new window function provides less resolution loss (i.e. azimuth resolution loss is 33.34% and range resolution loss is 36.58%) than conventional window functions (i.e. Hamming, Hanning etc.). Conventional linear window function is not suitable for UWB SAR image formation. They can suppress sidelobes level but accompanies with resolution loss. But this new window function is able to control both orthogonal and non-orthogonal sidelobes at the desired level and also preserves the spatial resolution at the same time. This apodization method has proved correct with a real SAR image.


## ACKNOWLEDGMENT

The author would like to thanks Blekinge Institute of Technology for providing the opportunity to do this research work, FOI (Swedish Defiance Research Agency) for providing SAR real image and also would like to express gratitude to Thomas Sjögren for guiding in the entire research work.

## REFERENCES


[1] Thomas G., Flores B.C., and Jae Sok-Son, "SAR sidelobe apodization using the Kaiser window", *Proceeding of the 2000 International Conference on image processing*, Vol. 1, pp. 709-712, 2000.

[2] Marco Schwerdt, "Calibration/Verification Concept of TerraSAR-X", *Science Team Meeting*, 2005.

[3] V. T. Vu, T. K. Sjögren, M. I. Pettersson, and H. Hellsten, "An Iimpulse response function for evaluation of ultrawideband SAR imaging," *IEEE Transactions on Signal Processing,* April 2010.

[4] T. K. Sjögren, V. T. Vu, and M. I. Pettersson, "2D apodization in UWB SAR using linear filtering," in *Proc. IEEE IGARSS'2011*, Vancouver, Canada, pp. 1689–1692, Jul. 2011.

[5] Meadows, and Patricia Wright, "ASAR IMP Image Quality (VV Polarisation)", 2002.

[6] V. T. Vu, T. K. Sjögren, and M. I. Pettersson, "On apodization techniques for ultra-wideband SAR imaging," *in Proc. EURAD' 2009*, Roma, Italy, pp. 529-532, Sep. 2009.